LAWRENCE
LIVERMORE
NATIONAL
LABORATORY

LLNL-PROC-417160

Developing The Physics Desing for NDCS-II, A Unique Pulse-Compressing Ion Accelerator

A. Friedman, J. J. Barnard, R. H. Cohen, D. P. Grote, S. M. Lund, W. M. Sharp, A. Faltens, E. Henestroza, J-Y. Jung, J. W. Kwan, E. P. Lee, M. A. Leitner, B. G. Logan, J. -L. Vay, W. L. Waldron, R. C. Davidson, M. Dorf, E. P. Gilson, I. Kaganovich

September 25, 2009

ICAP 2009
San Francisco, CA, United States
August 31, 2009 through September 4, 2009

Disclaimer

DEVELOPING THE PHYSICS DESIGN FOR NDCX-II, A UNIQUE PULSE-COMPRESSING ION ACCELERATOR*

A. Friedman, J. J. Barnard, R. H. Cohen, D. P. Grote, S. M. Lund, W. M. Sharp, LLNL, USA
A. Faltens, E. Henestroza, J-Y. Jung, J. W. Kwan, E. P. Lee, M. A. Leitner, B. G. Logan,
J.-L. Vay, W. L. Waldron, LBNL, USA
R. C. Davidson, M. Dorf, E. P. Gilson, I. Kaganovich, PPPL, USA

Abstract

The Heavy Ion Fusion Science Virtual National Laboratory (a collaboration of LBNL, LLNL, and PPPL) is using intense ion beams to heat thin foils to the "warm dense matter" regime at $\lesssim 1$ eV, and is developing capabilities for studying target physics relevant to ion-driven inertial fusion energy. The need for rapid target heating led to the development of plasma-neutralized pulse compression, with current amplification factors exceeding 50 now routine on the Neutralized Drift Compression Experiment (NDCX). Construction of an improved platform, NDCX-II, has begun at LBNL with planned completion in 2012. Using refurbished induction cells from the Advanced Test Accelerator at LLNL, NDCX-II will compress a ~500 ns pulse of Li^+ ions to ~1 ns while accelerating it to 3-4 MeV over ~15 m. Strong space charge forces are incorporated into the machine design at a fundamental level. We are using analysis, an interactive 1D PIC code (ASP) with optimizing capabilities and centroid tracking, and multi-dimensional Warp-code PIC simulations, to develop the NDCX-II accelerator. This paper describes the computational models employed, and the resulting physics design for the accelerator.

INTRODUCTION

The Heavy Ion Fusion Science Virtual National Laboratory (HIFS-VNL) is a collaboration of Lawrence Berkeley National Laboratory, Lawrence Livermore National Laboratory, and the Princeton Plasma Physics Laboratory. The VNL is using intense ion beams to enable the study of matter in the poorly-understood "warm dense matter" (WDM) regime at $\lesssim$1 eV, and is developing capabilities for experimental studies of inertial-fusion target physics relevant to ion-driven inertial fusion energy. For an overview, see [1].

The need for rapid target heating motivated the development of ion beam compression in the presence of a neutralizing plasma (which serves to minimize the beam space-charge forces that otherwise would inhibit compression to a compact volume). Bunching factors exceeding 50 have been achieved on the Neutralized Drift Compression Experiment (NDCX) at LBNL. Funding for an improved research platform, NDCX-II, has been approved (via the American Recovery and Reinvestment Act of 2009) and construction is beginning at LBNL, with planned completion in 2012. This will be the first ion induction accelerator specifically designed to heat targets with short pulses. Using refurbished induction cells, Blumlein voltage sources, and transmission lines from the decommissioned Advanced Test Accelerator (ATA) at LLNL, NDCX-II will compress a ~1 m, ~500 ns pulse of Li^+ ions to ~1 cm, ~1 ns while accelerating it to 3-4 MeV over ~15 m. This is accomplished in two stages: the induction accelerator itself, which shortens the pulse to ~0.2 m, 20 ns (~5x increased speed and ~5x decreased length); and a downstream neutralized drift compression line, which enables the final compression (spatial and temporal) through a factor of ~20 or more. The layout is shown in Fig. 1.

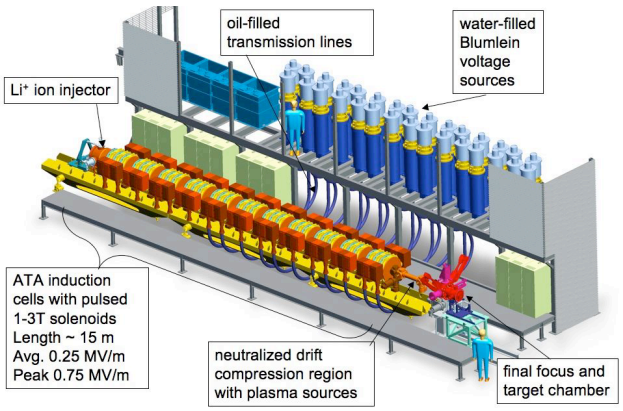

Figure 1: CAD rendering of a design concept for NDCX-II.

The ferrite in each ATA cell offers 0.014 V-s of flux swing, while the Blumleins can source as much as 250 kV with a FWHM of 70 ns. Passive pulse-shaping elements can be inserted into the "compensation boxes" attached to each cell, offering some flexibility in the accelerating waveforms. It is possible to generate longer pulses (and necessary to do so at the front end of the machine), as well as pulses with waveforms optimized to confine the beam-ends, but the need to minimize costs motivates keeping the voltage of any new power supplies to 100 kV or less. The NDCX-II lattice period is unchanged from that of the ATA, at 0.28 m; the accelerating gaps (across which the driving inductive electric field appears) are 2.8 cm long. Because ions do not rapidly reach high speeds, transverse confinement of the beam against its own space charge requires that the existing DC solenoids be replaced by much stronger pulsed solenoids with fields approaching 3 T.

For three reasons, it will be necessary to rebuild the radially innermost parts of the ATA cells. Firstly, a major

* This work was performed under the auspices of the USDOE by LLNL under Contract DE-AC52-07NA27344, by LBNL under Contract DE-AC02-05CH11231, and by PPPL under Contract DE-AC02-76CH03073.

loss of Volt-seconds available for acceleration results when the return flux of a pulsed solenoid passes through a ferromagnetic core. Thus, we plan to introduce extra magnetic elements (a copper layer, magnetic iron, or a secondary winding) outboard of each solenoid, to force flux to return inboard of the ferrite. This requires reducing the original 6.7 cm ATA beam-pipe radius to 4.5 cm. Secondly, an accelerating gap must be "on" while any of the beam overlaps its fringe field; the transit time for a single particle can be comparable to the time for the beam to pass a fixed axial position z. To shorten this fringe, it is again necessary to reduce the pipe radius (or at least the radius of the conductor that sets the axial scale of the fringe field) to of order 4 or 4.5 cm. Finally, the ATA cells contain end plates that allow large eddy currents; these plates will be made thinner.

Non-relativistic ions exhibit complex dynamics, more so when the beam is space-charge-dominated longitudinally and transversely. The beam manipulations in NDCX-II are actually enabled by longitudinal space charge forces. We are using analysis, an interactive 1D PIC code (ASP) with optimizing capabilities and a centroid-offset model, and both (r, z) and 3D Warp [2] simulations, to develop the NDCX-II accelerator. This paper describes the computational models used for these studies, and the resulting physics design. A companion paper [3], and earlier papers on this work [4, 5, 6], provide complementary information.

1-D ASP CODE MODEL

The ASP code (an acronym for "Acceleration Schedule Program") follows the beam's evolving longitudinal phase space (z, v_z), and was developed to facilitate the synthesis and optimization of accleration schedules. It uses well-established particle-in-cell methods, but solves for the space-charge field with a modified 1-D Poisson formulation [7]. In order to capture the fall-off with axial distance of a beam slice's influence (associated with image charges in the beam pipe wall), we use the following prescription for the electrostatic potential $\phi(z)$:

$$\nabla^2\phi \simeq \frac{d^2\phi}{dz^2} - k_\perp^2\,\phi = -\frac{\rho}{\epsilon_0}\ , \qquad (1)$$

where the transverse inverse scale length $k_\perp$ is defined by:

$$k_\perp^2 = 4/(g_0 r_b^2)\ ; \qquad g_0 = 2\ln(r_w/r_b)\ . \qquad (2)$$

Here, r_b is the nominal beam radius, r_w is the pipe ("wall") radius, and the so-called "g-factor" g_0 has been introduced to make correspondence with the long-wavelength limit. For very short wavelength variations the effect of the $k_\perp^2$ term is properly small, while at long wavelengths the electric field is given by

$$E_z = -\frac{\partial\phi}{\partial z} = -\frac{g_0}{4\pi\epsilon_0}\frac{d}{dz}(\pi r_b^2\rho) = -\frac{g_0}{4\pi\epsilon_0}\frac{d\lambda(z)}{dz}\ , \qquad (3)$$

where $\lambda(z)$ is the line charge density (C/m) [7, 8]. Our prescription for g_0 differs slightly from that of [7] because we seek to model a space-charge-dominated beam of roughly constant density, that is, $\lambda(z) \propto r_b^2(z)$. In practice, comparisons with (r, z) Warp calculations allow us to set g_0.

ASP represents the accelerating-gap fields $E_{z,i}(z, t)$ due to each time-varying gap voltage $V_i(t)$ via the "Lee" model [9]; we use the single-term approximation (Eq. A7 of the reference) because the gap is narrow.

The general "type" of each accelerating waveform (including ideal ramps or flat-tops, circuit-models of various kinds, and self-adjusting "ear" waveforms that counteract beam end expansion) is set by the user. The code automatically adjusts each waveform using estimated times of beam entry into and exit from the gap's fringe field, constrained by user-specified limits to peak voltage and Volt-seconds.

In addition to the longitudinal phase-space coordinates (z_k, p_{zk}) of each simulation particle (beam slice) k, ASP also tracks the transverse coordinates $(x_k, y_k, p_{xk}, p_{yk})$ of its centroid. In a perfectly aligned system, all of these would remain zero. However, misalignments drive the beam off axis. Furthermore, because of the head-to-tail energy variation along the beam, once a displacement occurs the different beam slices gyrate in the solenoids' field at their own peculiar rates. The result is a "corkscrew" distortion [10]. Fortunately, methods for minimizing its amplitude have been developed for electron linacs [11] , and our studies (described below) show that they remain effective for NDCX-II with its large energy variation.

ASP was designed to be interactive; it is written in the Python scripting language, with a few computationally-intensive routines in Fortran. A few hundred simulation particles (beam slices) are used, and a run without iterations takes a few minutes on a single processor. Iterations of two kinds are routinely carried out: variations of the applied voltage waveforms $V_i(t)$ to establish the acceleration schedule, and iterative tuning of the "steering" dipole magnet strengths to minimize the beam's corkscrew and off-axis shift. On a 4-processor computational node of a 2.2 GHz AMD Linux cluster, each "steering" run takes between two and three hours. Using a script which launches four jobs at a time, an ensemble of 20 cases with differing random alignment errors runs overnight.

In order to initialize the ASP beam, we begin by carrying out a Warp simulation of the source diode and matching section, and record the beam parameters as it passes through a plane upstream of the first gap; we then construct a smooth beam in ASP that resembles the Warp beam, using a simple parameterization. This method requires manual intervention and is crude, but works well enough. We have most recently implemented a method that uses the Warp data to construct a profile which is then used as the basis in detail for the ASP initial beam [3].

1-D PHYSICS DESIGN

We identified two principles which served as guides to development of an effective acceleration schedule. The first of these is to "shorten the beam first" (compress it longitu-

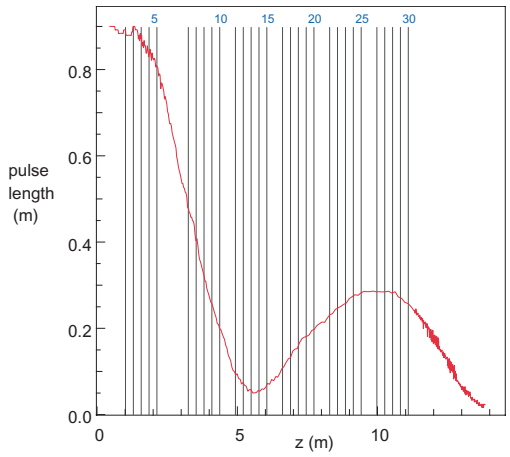

Figure 2: Pulse length vs. axial coordinate z. Numbers label the accelerating gaps.

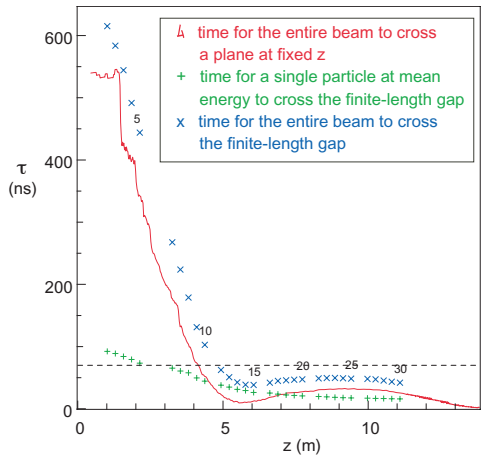

Figure 3: Pulse duration vs. z; the key time is that for the entire beam to traverse a gap's fringe field from entrance to exit.

dinally before the main acceleration) via a process of non-neutral drift compression. We use the initial cells primarily to impose a velocity tilt, while others provide longitudinal control; space is left for the drift compression. The goal is to achieve a sub-70 ns beam transit time through the acceleration gaps (including their fringe fields) as early as possible, so that we can use as many Blumlein-driven 200-kV pulses as possible. It is necessary, at this stage, to compress the beam carefully so as to minimize the effects of space charge which might lead to beam non-uniformity. Thus we seek to achieve (ideally) a large linear velocity "tilt" with $v_z(z) \propto z$ and a smooth density profile. We obtain the desired waveforms using a least-squares optimization that penalizes both nonlinearity and nonuniformity.

The second guiding principle is to "let the beam bounce." Rapid inward motion in the beam frame is required to reduce the pulse duration below 70 ns. Space charge ultimately inhibits this compression. At that point, the beam is shorter than the fringe field of a gap, and is not sustainable because confining fields are ineffective. Thus, the beam "bounces" — that is, it starts to lengthen. Nonetheless, the duration remains below 70 ns because it is now moving faster and is confined by additional ramped pulses. We allow it to lengthen while applying additional acceleration via flat-top pulses, and longitudinal confinement via ramped ("triangular") pulses. Alternatively, trapezoidal pulses may be used instead of a combination of flat-tops and triangles. The final few gaps apply the velocity tilt for neutralized drift compression onto the target.

Figure 2 shows the evolution of the beam length, while Fig. 3 shows the evolution of the pulse duration. While the design has yet to be finalized, the system described here is representative, with the final ∼20 induction cells driven by the ATA Blumleins and the rest by lower-voltage sources. Most of the required waveforms (shown in Fig. 4) are simple enough to be formed with passive circuits in the "compensation boxes" that are attached to the ATA cells. ASP solves simplified circuit equations for the 200 kV triangular pulses; laboratory tests of such pulse shaping are underway, and to date a high-quality ∼60 ns ramp has been achieved (our latest ASP runs use this experimental data). Similar circuits may be able to form the initial tilt-generating waveforms. The low-voltage highly shaped "ear" waveforms that provide beam-end control (shown in black in Fig. 4) will be driven by programmable circuits.

Figure 5 shows the evolution of the phase space and current. The final panel shows the beam when its centroid is at the plane of best longitudinal focus. This plane is estimated by an RMS measure [12] and refined by searching for that plane through which the most current flows in a 1-ns window. In ASP, the beam is assumed perfectly neutralized after it exits the accelerator (the space-charge field is ramped to zero over a user-specified length).

(R, Z) SIMULATIONS

As mentioned earlier, we are carrying out both (r, z) and full 3-D simulations of NDCX-II using the Warp code. These simulations include detailed acceleration gaps and

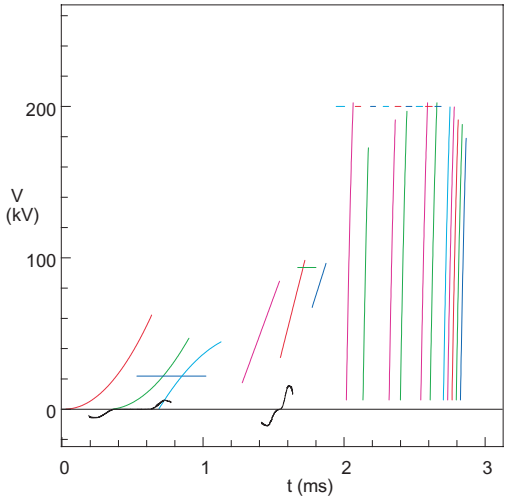

Figure 4: Waveforms for accelerattion as developed via ASP.

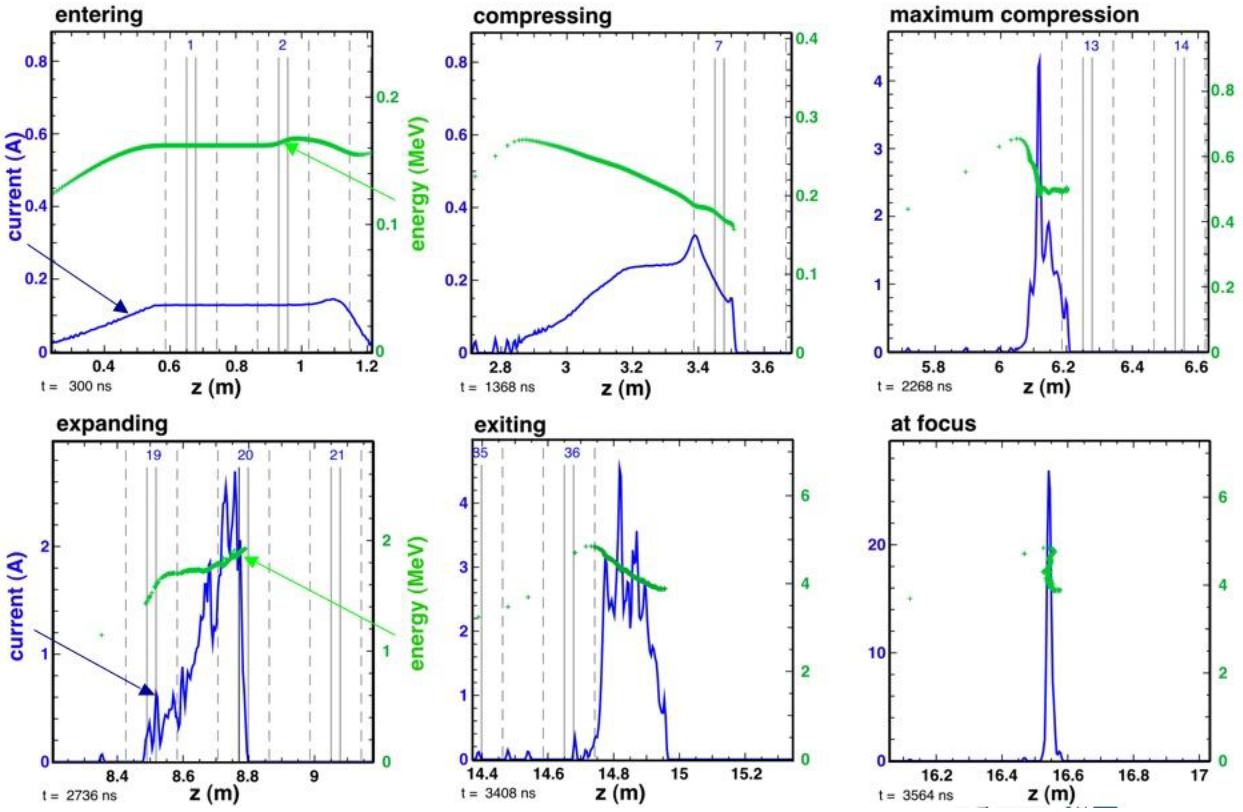

Figure 5: ASP snapshots.

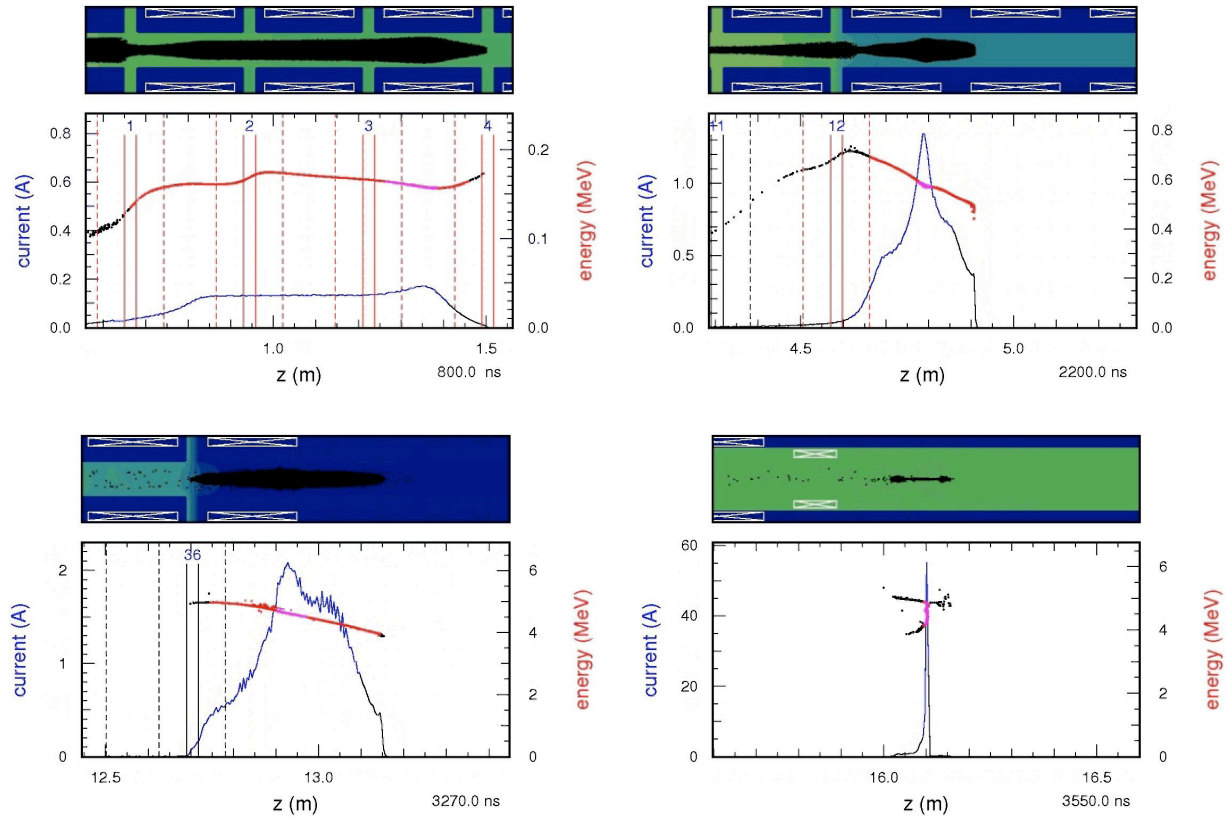

Figure 6: Warp RZ snapshots.

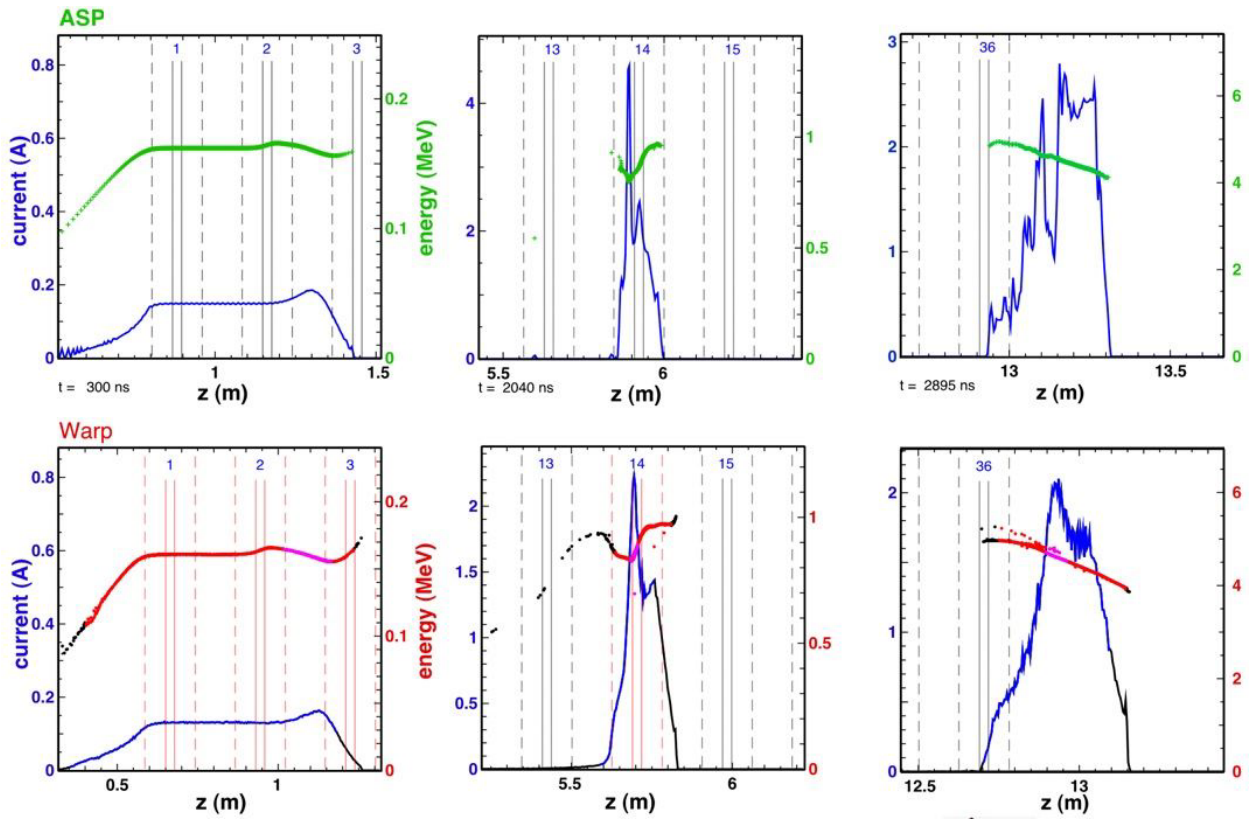

Figure 7: ASP vs. Warp comparison.

focusing magnet fields, and solve for the beam self-field in a conducting pipe. The gap fields have a two-dimensional variation (that is, the fringe field has reduced axial extent at larger radius); we derive these fields by solving Laplace's equation with differing potential on the walls at each side of the gap; the true field is inductive, but for these slowly varying fields the approximation is excellent. As an example, Fig. 6 shows a few snapshots from a Warp movie; the elevation view does not clearly convey the compactness of the beam, which has a long, low-density tail. (A number of such movies may be found at [13].) In view of the radial variation of the gap field and the approximate nature of the 1-D self-field, it was not clear at the outset that a set of waveforms developed in ASP would be effective in accelerating, confining, and compressing the Warp beam. We were pleased to see that indeed our design procedure works reliably provided the initial beam is well described in ASP (see Fig. 7), and efficiently relative to iterative Warp runs.

The (r, z) mode of Warp is also used to design the injector (Fig. 8). For scoping we are using one refinement patch around the emitter; to obtain converged voltage waveforms it will be important to use fully adaptive multi-level AMR.

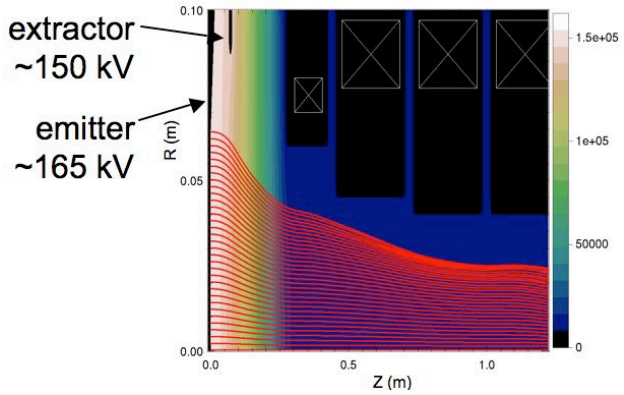

Figure 8: Warp simulation of a possible injector configuration.

3-D EFFECTS: MISALIGNMENTS, CORKSCREW, AND THEIR MITIGATION

With nominal random solenoid-end misalignments of up to 0.5 mm (thus allowing for transverse offsets as well as pitch and yaw tilts), both ASP and Warp simulations indicate good beam transmission through the accelerator. See the 3-D Warp movie with random 1-mm shifts of solenoid ends at [13]. 3-D Warp simulations show that the degradation of the focal intensity is smooth, and modest for small errors. Nonetheless, it is highly desirable to use steering dipole magnets to minimize both the corkscrew amplitude and the off-axis displacement. In Fig. 9 we show how iterative dipole tuning can be effective in such a system. The most recent designs for NDCX-II are built around blocks of three cells, followed by a non-accelerating lattice period with a solenoid, steering dipoles for x and y, and diagnostics to measure the beam centroid displacement.

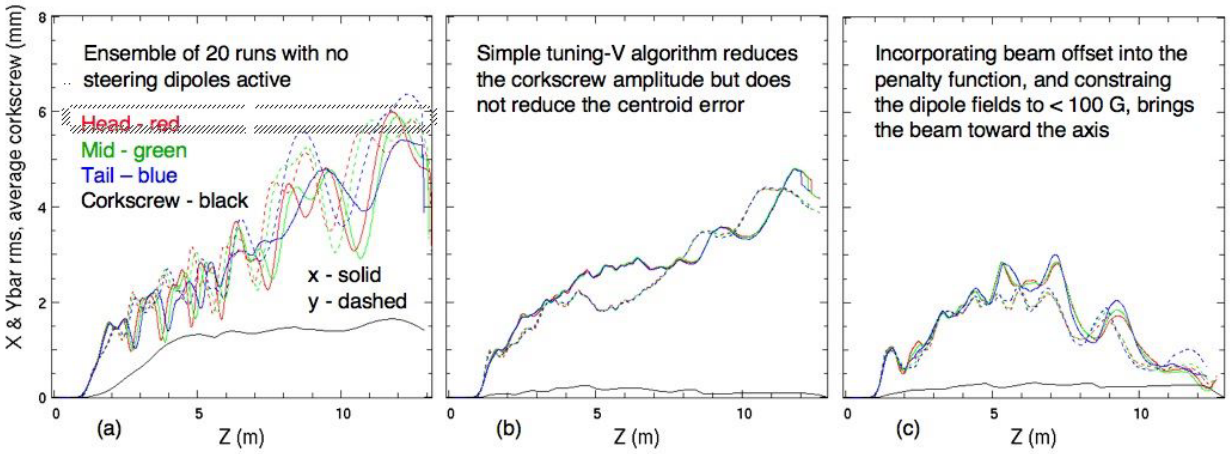

Figure 9: ASP studies of steering, showing RMS of x and y centroid coordinates vs. z for head, middle, and tail particles, and the corkscrew amplitude; the results are averages over 20 simulations with differing random offsets of solenoid ends up to 1 mm. The penalty function was evaluated at the next sensor downstream from the dipole being varied.

DISCUSSION

We have developed the physics design for a novel accelerator, using a new computational tool (ASP) in tandem with an existing tool (Warp). Computational aspects of this work, including the 1-D field solution with tuned axial falloff, self-adjusting waveforms that make maximal use of available volt-seconds and voltage, iterations for waveform design and for beam steering, and the interactive very-high-level code framework based on Python, have all worked out well in this application.

The baseline design for the NDCX-II project will be established later this year; it will resemble the designs shown here, but should take the beam to a lower final kinetic energy (the goal for the WDM application is a mean kinetic energy of 2.8 MeV, as appropriate for uniform heating by a beam that slows through the Bragg peak in a foil target).

This paper has described the physics design of the NDCX-II accelerator, and has not attempted to cover many other important aspects of the full machine, which include the ion source and the pulsed power, as well as the neutralized drift line, final focusing solenoid, and target chamber (into all of which which plasma must be injected at sufficient density that the beam space charge is uniformly cancelled). For discussion of these topics the reader may refer to the Proceedings of the recent Heavy Ion Fusion Symposium [14] and presentations at PAC09 [15, 16].

REFERENCES

[1] B. G. Logan, *et al.*, *Nucl. Instr. and Meth.* **A 577**, 1 (2007).

[2] D.P. Grote, A. Friedman, I. Haber, W. Fawley, J.-L. Vay, *Nucl. Instr. and Meth.* **A 415**, 428 (1998).

[3] W. M. Sharp, A. Friedman, D. P. Grote, R. H. Cohen, S. M. Lund, M. Leitner, J.-L. Vay, and W. L. Waldron, "Modeling the NDCX-II Physics Design," ICAP'09, San Francisco, Sept. 2009, `http://www.JACoW.org` (these *Proceedings*).

[4] A. Friedman, et al., *Nucl. Instr. and Meth.* **A 606**, 6 (2009).

[5] W. M. Sharp, A. Friedman, D.P. Grote, E. Henestroza, M. A. Leitner, and W. L. Waldron, *Nucl. Instr. and Meth.* **A 606**, 97 (2009).

[6] W. M. Sharp, A. Friedman, D.P. Grote, E. Henestroza, M. A. Leitner, and W. L. Waldron, "Simulating an Acceleration Schedule for NDCX-II," PAC'09, Vancouver, May 2009, TH5PFP072, `http://www.JACoW.org`.

[7] J. J. Barnard, G. J. Caporaso, S. S. Yu, and S. Eylon, "One Dimensional Simulations of Transients in Heavy Ion Injectors," PAC'93, Washington, DC, May 1993, pp. 712-714, `http://www.JACoW.org`.

[8] J. J. Barnard and S. M. Lund, Course notes, *Beam Physics with Intense Space-Charge*, U.S. Particle Accelerator School, Univ. of Maryland, June 2008, Pp. 13-14 of Section on *Longitudinal Physics Part II*, `http://uspas.fnal.gov/materials/08UMD/BeamPhysics.html`

[9] E. P. Lee (private communication); see: D. R. Welch, *et al.*, *Phys. Rev. ST Accel. Beams* **11**, 064701 (2008), Appen. A.

[10] Y-J. Chen, *Nucl. Instr. and Meth.* **A 292**, 455 (1990).

[11] Y-J. Chen, *Nucl. Instr. and Meth.* **A 398**, 139 (1997).

[12] A. Friedman, "Some kinematic aspects of neutralized drift compression," LLNL Note LLNL-TR-402447, March 2008.

[13] `http://hifweb.lbl.gov/public/movies/ICAP09`

[14] *Proc. 17th Int. Sympos. on Heavy Ion Inertial Fusion (HIF2008)*, Tokyo, Aug. 4-9, 2008, published as Nucl. Instr. and Meth. A 606, (2009).

[15] I. D. Kaganovich, et al., "Designing Neutralized Drift Compression for Focusing of Intense Ion Beam Pulses in Background Plasma" PAC'09, Vancouver, May 2009, `http://www.JACoW.org`.

[16] R. C. Davidson, E. A. Startsev, M. Dorf, I. D. Kaganovich and H. Qin, "Collective Instabilities and Beam-Plasma Interactions for an Intense Ion Beam Propagating through Background Plasma," PAC'09, Vancouver, May 2009, `http://www.JACoW.org`.